MCB
Journals.ASM.org

Loss of Akt1 in Mice Increases Energy Expenditure and Protects against Diet-Induced Obesity

Min Wan,[a] Rachael M. Easton,[a]* Catherine E. Gleason,[a]* Bobby R. Monks,[a] Kohjiro Ueki,[b] C. Ronald Kahn,[c] and Morris J. Birnbaum[a]

The Institute for Diabetes, Obesity, and Metabolism, University of Pennsylvania, Philadelphia, Pennsylvania, USA[a]; Graduate School of Medicine, The University of Tokyo, Tokyo, Japan[b]; and Research Division, Joslin Diabetes Center, Harvard Medical School, Boston, Massachusetts, USA[c]

Akt is encoded by a gene family for which each isoform serves distinct but overlapping functions. Based on the phenotypes of the germ line gene disruptions, Akt1 has been associated with control of growth, whereas Akt2 has been linked to metabolic regulation. Here we show that Akt1 serves an unexpected role in the regulation of energy metabolism, as mice deficient for *Akt1* exhibit protection from diet-induced obesity and its associated insulin resistance. Although skeletal muscle contributes most of the resting and exercising energy expenditure, muscle-specific deletion of *Akt1* does not recapitulate the phenotype, indicating that the role of Akt1 in skeletal muscle is cell nonautonomous. These data indicate a previously unknown function of Akt1 in energy metabolism and provide a novel target for treatment of obesity.

Obesity has become a worldwide health problem, largely due to its health care costs as well as associated complications, like cardiovascular disease, cancer, and type II diabetes. Many ongoing studies have been directed toward preventing and treating obesity, although thus far most of the positive responses have not been long-lasting. The maintenance of a stable body weight requires a delicate balance between food intake and energy expenditure, which is easily disrupted in people enjoying the modern diet and a sedentary lifestyle and with a predisposing genetic make-up. Reduced physical activity and lower energy expenditure are associated with weight gain in human subjects (19, 35, 37). Lean mass, mostly skeletal muscle, contributes most of the resting and exercising energy expenditure (4). With the advent of the ability to manipulate the mouse genome, the identification of genes determining energy expenditure and body mass has become feasible and is being studied intensively. One mechanism that has been suggested to increase basal metabolic rate and afford protection from diet-induced obesity in mice is a stimulated mitochondrial biogenesis and increased respiratory uncoupling in skeletal muscle (9–11, 29, 39).

The serine-threonine protein kinase family Akt, also known as protein kinase B (PKB), is comprised of three isoforms, Akt1/PKBα, Akt2/PKBβ, and Akt3/PKBγ, each encoded by a distinct gene (40). All three members have been ablated in mice individually or in combination by our group and others (16). Akt1 is expressed ubiquitously, and its knockout shows no compensatory elevation of Akt2 expression and results in smaller body size and growth retardation with normal glucose homeostasis (6, 8). Akt2 is expressed primarily in insulin-responsive tissues, like liver, skeletal muscle, and adipose tissues (7). Genetic ablation of *Akt2* in mice results in a diabetes-like phenotype that includes impaired glucose tolerance, reduced insulin-dependent glucose uptake in muscle and adipose tissue, and increased hepatic glucose production as determined by studies employing a euglycemic-hyperinsulinemic clamp (7, 14). Recent studies also showed that deletion of *Akt2* in liver ameliorated hepatic steatosis in several obese mouse models (20, 24, 38). Akt3 is expressed predominantly in brain and testes, and germ line deletion of *Akt3* in mice causes a reduction in brain size without affecting glucose homeostasis (13). Taken together, these data suggest that Akt2 is most important to the regulation of metabolism, whereas Akt1 is critical to growth control, although there are many reports indicating overlapping functions among Akt isoforms (5, 12, 14, 31, 41). For example, in 2010, Buzzi et al. reported that *Akt1* knockout mice have improved insulin sensitivity and elevated insulin secretion, potentially as a result of decreased insulin receptor substrate 2 (IRS2) signaling in pancreatic β cells, which argues for a metabolic role of Akt1 in mice (5).

In our original description of the phenotypes of *Akt1* null ($Akt1^{-/-}$) mice, we noted a trend toward improved glucose tolerance that did not achieve statistical significance (8). In order to stress the system and possibly elicit a more striking indication for a role for Akt1 in metabolic control, we placed $Akt1^{-/-}$ mice on a high-fat diet (HFD). Surprisingly, mice with deletion of *Akt1* were protected from diet-induced obesity and its associated insulin resistance. In this paper, we describe the analysis of this phenotype and report an increase in energy expenditure resulting from germ line deletion of *Akt1*.

MATERIALS AND METHODS

Animals. $Akt1^{-/-}$ mice were backcrossed >10 generations to C57BL/6J mice from Jackson Laboratory (8). *ob/ob* mice were purchased from Jackson laboratory. $Akt1^{loxP/loxP}$ mice were generated by first obtaining the *Akt1* gene spanning from intron 3 to intron 13 via screening of a mouse genomic library (lambda FIXII Library; Stratagene). After digestion with SmaI and HindIII, a 1.5-kb fragment of intron 3 was treated with Klenow enzyme and subcloned into the preblunted XbaI site of the *loxP*-flanked neomycin resistance/thymidine kinase selection cassette vector (pInt3Akt1-loxPneo/TK). A 1.5-kb fragment, which spanned intron 3 to intron 5 and was obtained from *Akt1* genomic DNA by digestion with

Received 14 June 2011 Returned for modification 15 July 2011
Accepted 19 October 2011
Published ahead of print 28 October 2011
Address correspondence to Morris J. Birnbaum, birnbaum@mail.med.upenn.edu.
* Present address: R. M. Easton: CSL Behring, King of Prussia, Pennsylvania, USA; C. E. Gleason: University of California, San Francisco, San Francisco, California, USA.

doi:10.1128/MCB.05806-11

HindIII, was treatment with Klenow enzyme and subcloned into the *loxP* cassette vector (plox-Akt1ex4-5). A 3-kb fragment obtained from *Akt1* genomic DNA by digestion with HindIII and SstI, which spanned intron 5 to intron 12, was treated with Klenow enzyme and inserted into the preblunted ClaI site of plox-Akt1ex4-5 (plox-Akt1ex4-12). After digesting plox-Akt1ex4-12 with SalI and HindIII, a 4.5-kb fragment was inserted between the SalI and HindIII sites of pInt3Akt1-loxPneo/TK. J1 embryonic stem cells were electroporated with 40 μg of the NotI-digested targeting vector and subjected to selection with G418, and the clones were screened for homologous recombination by PCR amplification of the intron 4 region and Southern blot analysis. Cells that were heterozygous for *loxP* sites flanking exons 3 and 4 of the *Akt1* gene were injected into blastocysts derived from C57BL/6J mice and implanted into pseudopregnant CD-1 foster mothers according to standard methods. Chimeric mice (>90% as judged by coat color) were then bred with C57BL/6J mice. *EIIa* > *Cre* mice were obtained from Klaus Kaestner, University of Pennsylvania. *Nestin* > *Cre* and *MCK* > *Cre* mice were purchased from Jackson Laboratory. Mice that were bred with *Cre* lines were of an FVB-C57BL/6J mixed background, and male littermates were used for all studies. Mice were maintained on a normal chow diet (laboratory rodent diet 5001; LabDiet) unless otherwise noted and kept under a 12-h light-dark cycle (7 a.m./7 p.m.) in a barrier facility. When fed the HFD (D12331i; Research Diets), mice were started on it at 4 to 5 weeks of age, continuing for 22 weeks.

Metabolic measurements. For glucose tolerance tests, mice were fasted overnight followed by oral gavage with 1 g/kg of body weight of glucose, and blood glucose levels were measured at the time points designated below.

Euglycemic-hyperinsulinemic clamping was performed by the Mouse Phenotyping, Physiology and Metabolism Core at the University of Pennsylvania. Wild-type (WT) and *Akt1*$^{-/-}$ mice were challenged on the HFD for 22 weeks before clamping. Mice were given a 10-mU/kg insulin bolus and then infused with 2.5 mU of insulin/kg/min. Blood glucose levels were maintained between 120 and 140 mg/dl.

Hepatic and serum triglyceride levels were measured as described previously (24). The measurements of other serum constituents were performed by the Radioimmunoassay and Biomarker Core (the Core) at the University of Pennsylvania.

Body composition, energy expenditure, locomotor activity, and food intake were analyzed by the Mouse Phenotyping, Physiology and Metabolism Core at the University of Pennsylvania. Body composition was determined by nuclear magnetic resonance (NMR) imaging analysis or dual-energy X-ray absorptiometry (DEXA), as noted below. Energy expenditure, locomotor activity, and food intake were assessed by using the Comprehensive Laboratory Animal Monitoring system (CLAMS). The respiratory exchange ratio (RER) was calculated as the volume of CO_2 versus volume of oxygen (VCO_2/VO_2) ratio. For fasting-feeding experiments, food was removed at 7:00 a.m., the start of the light cycle, and freely accessible from 7:00 p.m. to 7:00 a.m. the next day (the entire dark cycle). Mice were trained under these conditions for 7 days before being subjected to measurements at the Core facility. During the monitoring process, water was accessible at all times.

Muscle palmitate oxidation assay. Experimental procedures for the muscle palmitate oxidate assay were modified from those described in a previous report (18). Soleus muscles were quickly removed from overnight-fasted mice and incubated in 0.5 ml Krebs-Ringer bicarbonate buffer (Sigma) for 30 min in an oxygenated 37°C water bath. Then the muscles were transferred to incubation buffer with 0.2-μCi [^{3}H]palmitate and placed in small glass vials in an oxygenated 37°C shaking water bath for 1 h. At the end of the incubation, 0.4 ml buffer was removed from each vial and mixed with 0.4 ml cold 10% trichloroacetic acid (TCA) and centrifuged 10 min, and the supernatant was neutralized with NaOH. After neutralization, the medium was applied to an AGI-X8 resin column (Bio-Rad) to remove charged molecules, and the column contents were eluted with 2 ml H_2O into a scintillation vial. Blank control vials contained the same buffer without soleus tissue.

RNA isolation and gene expression analysis. For RNA isolation and gene expression analysis, total RNA was extracted from skeletal muscle by using TRIzol reagent (Invitrogen), reverse transcribed with random decamers in the RetroScript kit (Ambion), and analyzed by real-time PCR on an Mx3000P quantitative PCR system (Stratagene) as described before (24). Primer sequences are available upon request.

Western blotting. Mice were sacrificed by spinal dislocation, and tissue samples were removed, clamp-frozen in liquid nitrogen, and stored at −80°C until being processed as described before (24). Blots were probed for Akt1 (2976; Cell Signaling Technology), pAMPK T172 (2535; Cell Signaling Technology), tAMPKα (2603; Cell Signaling Technology), pACC (3661; Cell Signaling Technology), tubulin (2128; Cell Signaling Technology), UCP3 (UCP33-A; Alpha Diagnostic International), and β-actin (ab6276; Abcam). Blots were then probed with horseradish peroxidase (HRP)-conjugated secondary antibodies (Santa Cruz Biotechnology).

Statistics. All data are presented as means ± standard errors of the means (SEM). As noted in the figure legends, data were analyzed by using an unpaired Student *t* test with two-tailed analysis, a one-way analysis of variance (ANOVA) followed by the Bonferroni posttest, or a two-way ANOVA followed by the Bonferroni posttest.

RESULTS

***Akt1*$^{-/-}$ mice are protected from diet-induced obesity.** To assess a putative metabolic role for Akt1 in mice, we placed 4- to 5-week-old *Akt1*$^{-/-}$ mice on a high-fat diet for 22 weeks. During this period, wild-type controls (*Akt1*$^{+/+}$) gained significantly more weight than those fed a normal chow (NC) diet, but there was a smaller difference in body weights between *Akt1*$^{-/-}$ mice on the two diets (Fig. 1A, left). Body composition also differed between WT and *Akt1*$^{-/-}$ mice, as the latter had a decreased contribution from fat mass (Fig. 1A, right). Even on a normal chow diet, WT mice had a significantly lower proportion of body mass attributable to lean mass than *Akt1*$^{-/-}$ mice (Fig. 1A, right). These data suggest that *Akt1*$^{-/-}$ mice have an energy balance that is different from WT mice, although an interpretation of our findings is complicated somewhat by the smaller body sizes of *Akt1* null mice.

To further investigate the mechanism underlying the differences in body size and composition, we monitored the metabolic activities of these mice by using CLAMS. *Akt1*$^{-/-}$ mice fed NC or HFD consumed significantly greater O_2 and produced more CO_2 than WT controls (Fig. 1B and C and data not shown). The lean mass of animals represents the major contributor of energy expenditure (4), but when values were normalized to lean mass, *Akt1*$^{-/-}$ mice still displayed significantly increased O_2 consumption and CO_2 production on both the NC diet and HFD (Fig. 1C and data not shown). Heat production was also elevated in *Akt1*$^{-/-}$ mice compared to WT mice on either diet, whereas RER, locomotor activity, and food and water consumption were not significantly different (Fig. 1D and E and data not shown). These data demonstrate that *Akt1*$^{-/-}$ mice have higher catabolic rates and are resistant to diet-induced obesity than WT mice.

Although these mice were crossed more than 10 generations onto a C57BL/6J background, we were still concerned that cotransmission of a closely linked gene could be responsible for the altered energy metabolism. To exclude this possibility, we generated independent germ line *Akt1* null mice by crossing mice carrying *Cre* recombinase driven by an *EIIa* promoter with *Akt1*$^{loxP/loxP}$ mice (25). These mice were null for *Akt1*, as confirmed by genomic PCR and Western blotting (data not shown).

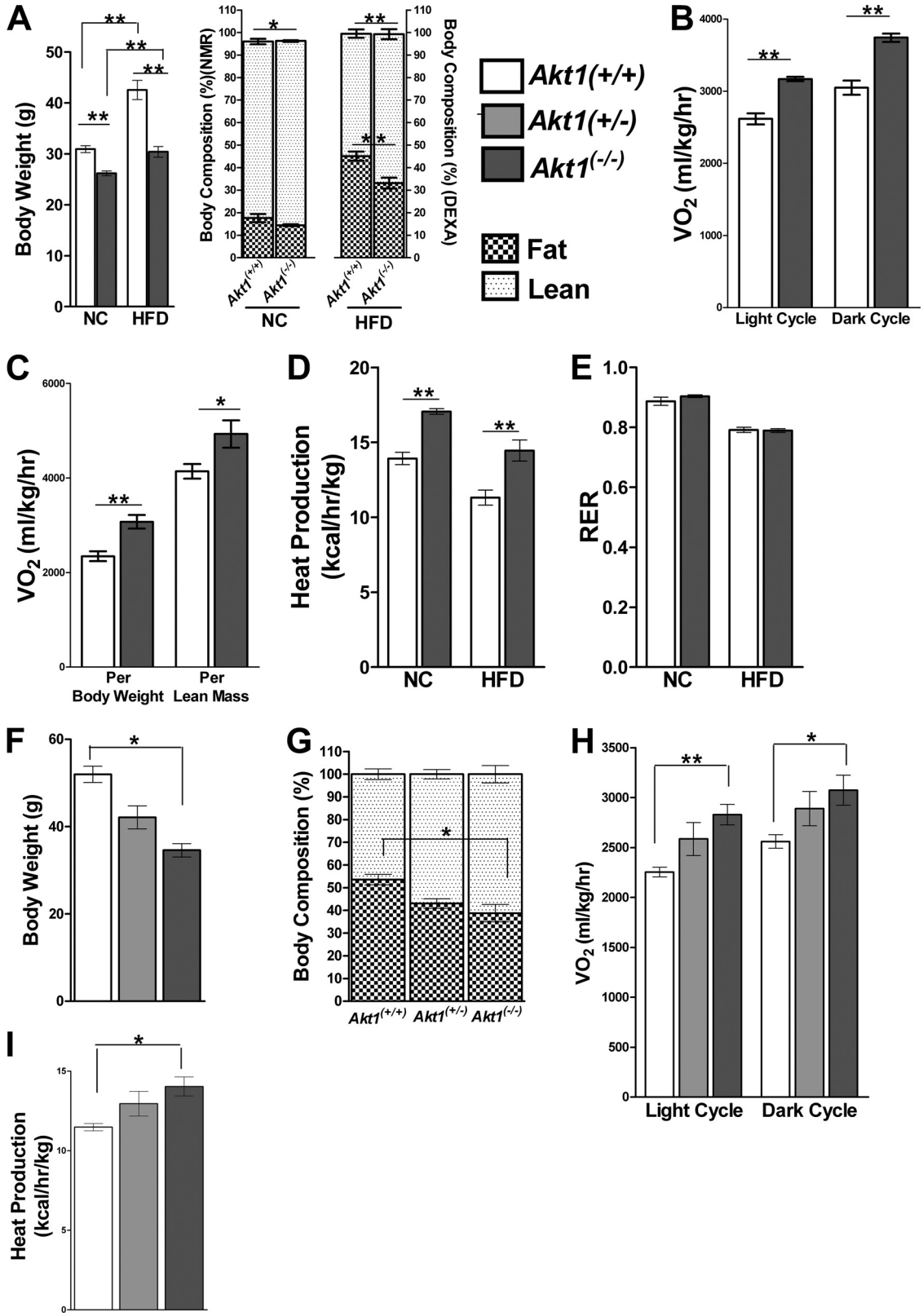

FIG 1 *Akt1*$^{-/-}$ mice are protected from diet-induced obesity. (A) Body weights and compositions of age-matched WT and *Akt1*$^{-/-}$ mice on NC or the HFD. For the NC group, body composition was determined by NMR analysis, energy expenditure was measured for 24 h, and mice were male and 7 months old ($n = 7$ to 9 mice). For the HFD group, body composition was determined by DEXA, energy expenditure was measured during the light cycle for 4 h, and mice were on HFD at 4 to 5 weeks of age and fed for 22 weeks ($n = 9$ to 10 animals for each genotype). *, $P < 0.05$; **, $P < 0.01$ by the Student *t* test. (B) O_2 consumptionof WT and *Akt1*$^{-/-}$ mice on NC. (C) O_2 consumption of WT and *Akt1*$^{-/-}$ mice on HFD. (D and E) Heat production and RER of WT and *Akt1*$^{-/-}$ mice on NC or HFD. *, $P < 0.05$; **, $P < 0.01$ by the Student *t* test. (F and G) Body weight and body composition by NMR for independently derived *Akt1*$^{+/+}$, *Akt1*$^{+/-}$, and *Akt1*$^{-/-}$ littermates after HFD feeding. (H and I) O_2 consumption and heat production of independently derived *Akt1*$^{+/+}$, *Akt1*$^{+/-}$, and *Akt1*$^{-/-}$ littermates after HFD feeding. Mice were fed the HFD for 22 weeks ($n = 4$ to 8 animals for each genotype). *, $P < 0.05$; **, $P < 0.01$ by one-way ANOVA followed by the Bonferroni posttest. All data are means ± SEM.

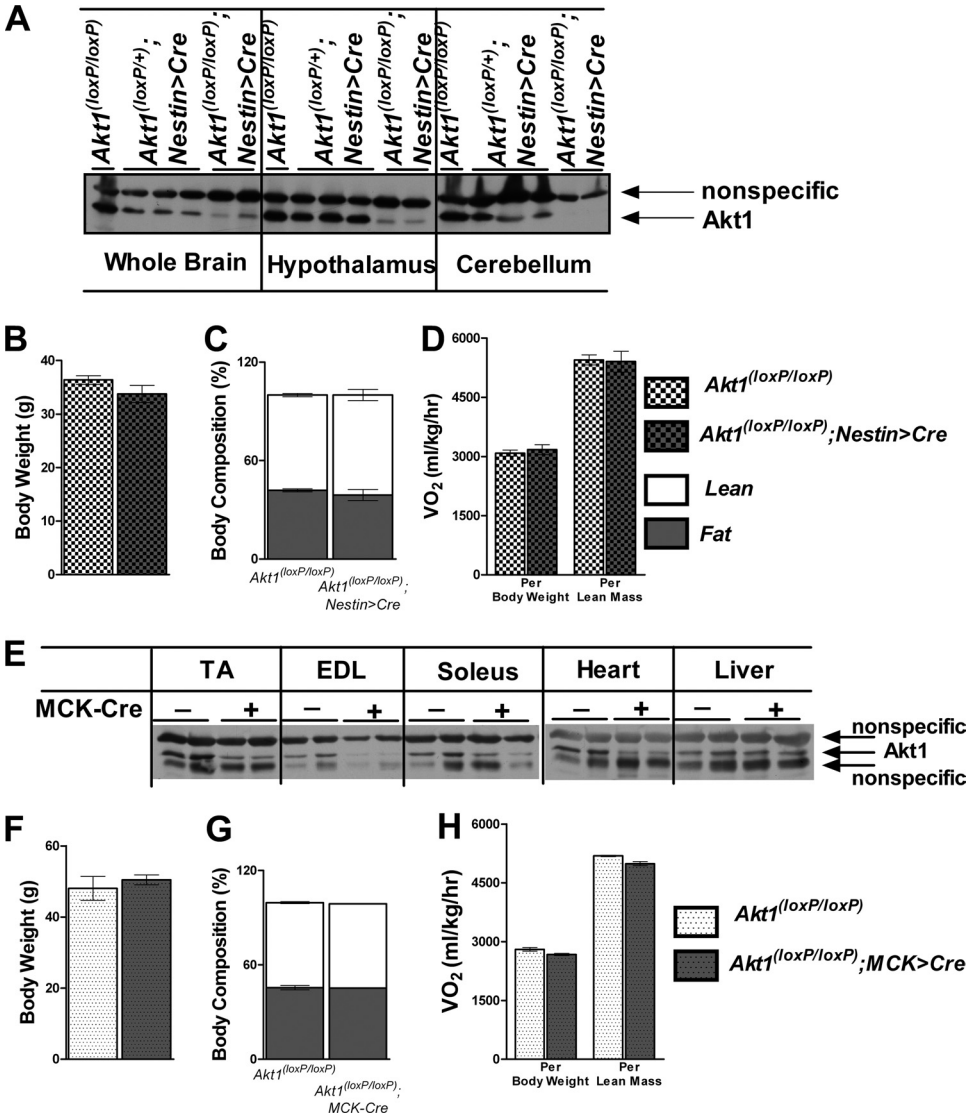

FIG 2 Deletion of Akt1 in Nestin or MCK-expressing cells does not prevent diet-induced obesity in mice. (A) Western blot showing the effects of deletion of Akt1 in *Akt1*$^{loxP/loxP}$; *Nestin* > *Cre* mice. Brain samples were from animals fed NC, and Akt1 levels were examined by Western blotting. Then, mice were fed the HFD for 22 weeks. (B to D) Body weight, body composition by NMR, and O_2 consumption for *Akt1*$^{loxP/loxP}$; *Nestin* > *Cre* mice and their littermate controls fed the HFD. Male mice started on the HFD when 4 weeks old and were maintained on it for 22 weeks before energy expenditure was measured ($n = 6$ for each group). (E) Western blot showing the effects of deletion of Akt1 in *Akt1*$^{loxP/loxP}$; *MCK* > *Cre* mice. Muscle samples were from animals fed NC, and Akt1 levels were examined by Western blotting. (F to H) Body weight, body composition by NMR, and O_2 consumption for *Akt1*$^{loxP/loxP}$; *MCK* > *Cre* mice and their littermate controls on the HFD. Male mice started on the HFD at 4 weeks of age and were maintained on it for 22 weeks before energy expenditure was measured ($n = 3$ animals for each group). EDL, extensor digitorum longus. All data are presented as means ± SEM.

After feeding these mice an HFD for 22 weeks, their body weights were significantly lower than their wild-type littermates, while the *Akt1*$^{+/-}$ mice displayed an intermediate phenotype (Fig. 1F). When we performed a replication of the experiment described above, the independently derived *Akt1*$^{-/-}$ mice displayed reduced adiposity after HFD challenge and elevated O_2 consumption and heat production (Fig. 1G to I). These data indicate that the altered energetic phenotypes were indeed caused by deletion of *Akt1*.

We next turned our attention to the identification of the tissue in which deletion of *Akt1* leads to the increased energy expenditure. Akt1 contributes about one-third of total Akt in the brain (13); we bred *Akt1*$^{loxP/loxP}$ mice with transgenic mice with *Cre* recombinase driven by a rat *Nestin* promoter and enhancer (*Nestin* > *Cre*), which led to efficient excision of brain Akt1 (Fig. 2A), and we challenged the animals with an HFD for 22 weeks. *Akt1*$^{loxP/loxP}$; *Nestin* > *Cre* mice did not reproduce the altered energy metabolism and protection diet-induced obesity of the *Akt1*$^{-/-}$ mice (Fig. 2B to D). Skeletal muscle represents the major contributor of energy expenditure (4); however, deletion of *Akt1* in skeletal muscle by *Cre* driven by the *muscle creatine kinase* promoter (*MCK* > *Cre*) did not recapitulate the effects of *Akt1* germ line deletion on body weight or energy expenditure (Fig. 2E to H). The liver also contributes to whole-body energy expenditure, but deletion of *Akt1* specifically in the liver, by breeding *Akt1*$^{loxP/loxP}$ mice to a *Cre* mouse line driven by an albumin promoter, did not phenocopy the *Akt1*$^{-/-}$ mice (data not shown).

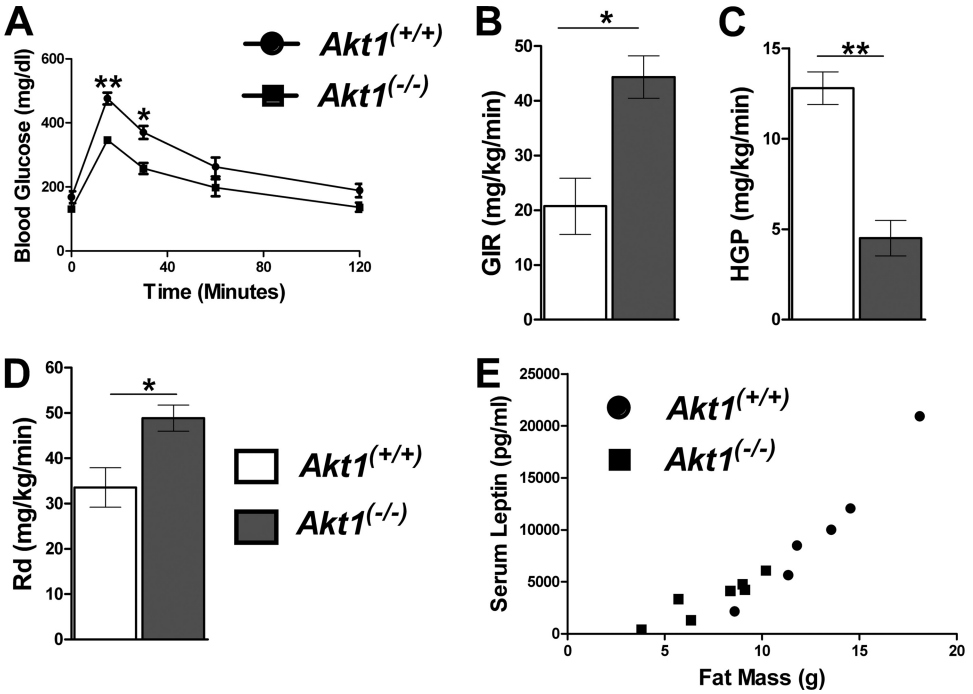

FIG 3 *Akt1*$^{-/-}$ mice have improved insulin sensitivity after HFD feeding compared to WT mice. (A) Glucose tolerance test. Mice were fed the HFD for 18 weeks, and 1 g of glucose/kg was orally administrated after overnight fasting ($n = 3$ to 4 animals for each group). The glucose infusion rate (GIR) (B), hepatic glucose production (HGP) (C), and peripheral glucose utilization rate (Rd) (D) during euglycemic-hyperinsulinemic clamping of mice fed the HFD for 22 weeks ($n = 3$ for each group) are shown. All data are presented as means ± SEM, *, $P < 0.05$; **, $P < 0.01$ by the Student *t* test. (E) Serum leptin levels after overnight fasting from mice fed an HFD for 22 weeks ($n = 6$ to 7 animals for each group). All data are presented as means ± SEM.

***Akt1*$^{-/-}$ mice on the HFD showed improved insulin sensitivity.** As shown in Fig. 3, when *Akt1*$^{-/-}$ mice were placed on the HFD, they demonstrated improved glucose tolerance and an increased glucose infusion rate upon euglycemic-hyperinsulinemic clamping compared to similarly fed WT mice (Fig. 3A and B). The latter was due to both a decrease in hepatic glucose production and an elevated peripheral glucose utilization rate (Rd) in *Akt1*$^{-/-}$ mice (Fig. 3C and D). *Akt1*$^{-/-}$ mice on an HFD had reduced leptin and total thyroxine and increased adiponectin in serum and no change in resistin levels (Table 1). The direct relationship between leptin and fat was preserved in *Akt1*$^{-/-}$ mice, consistent with the reduced leptin resulting directly from decreased adiposity (Fig. 3E). Deletion of *Akt1* also protected mice from steatosis when fed an HFD (Table 1).

TABLE 1 Metabolic characteristics of *Akt1*$^{-/-}$ mice on HFD

Parameter	Value for mouse genotype[a]	
	Akt1$^{+/+}$	Akt1$^{-/-}$
Fasted triglyceride (mg/dl)	50.624 ± 3.177	45.952 ± 3.285
Fed triglyceride (mg/dl)	69.720 ± 13.870	61.580 ± 18.770
Fasted insulin (ng/ml)	2.151 ± 0.577	1.632 ± 0.607
Fed insulin (ng/ml)	4.142 ± 2.908	2.900 ± 1.885
Fasted leptin (ng/ml)	9.882 ± 2.622	3.462 ± 0.750*
Fasted adiponectin (μg/ml)	8.618 ± 0.509	16.411 ± 0.997**
Fasted thyroxine (total T_4, in μg/dl)	3.740 ± 0.156	3.088 ± 0.137*
Fasted free fatty acid (mM)	1.106 ± 0.509	1.105 ± 0.150
Fasted β-hydroxybutyrate (mg/dl)	8.342 ± 1.694	6.491 ± 0.671
Fasted resistin (ng/ml)	1.640 ± 0.135	1.467 ± 0.353
Fasted liver triglyceride (mg/g of protein)	57.141 ± 10.698	33.479 ± 3.217*

[a] All data were obtained in overnight-fasted animals or fed animals as indicated and are presented as means ± SEM ($n = 4$ to 7 animals per group). *, $P < 0.05$; **, $P < 0.01$ (compared to WT using the Student *t* test).

Young *Akt1* knockout mice display an increased energy expenditure. In an attempt to determine whether the reduced adiposity in 7-month-old *Akt1*$^{-/-}$ mice was the cause or result of altered energy metabolism, we examined 10-week-old mice, an age when *Akt1*$^{-/-}$ mice were smaller than WT but had indistinguishable body compositions (Fig. 4A and B). Consistent with the results presented above, 24-h O_2 consumption and CO_2 production were increased in *Akt1*$^{-/-}$ mice (Fig. 4C and data not shown). Heat production was also significantly elevated in *Akt1*$^{-/-}$ mice (Fig. 4D). RER, food and water intake, and locomotor activity were not altered in *Akt1*$^{-/-}$ mice (Fig. 4E and data not shown). Similar phenotypes were observed for the independently derived line of *Akt1*$^{-/-}$ mice (data not shown). These data suggest that an increased energy expenditure is the primary cause of reduced adiposity in aged mice or mice fed a high-fat diet.

Weight-matched *Akt1*$^{-/-}$ mice showed elevated energy expenditures. As noted above, the smaller body size of *Akt1*$^{-/-}$ mice compared to their age-matched counterparts complicates the interpretation of the energetic phenotypes, even when the measurements are normalized to body or lean weight (4, 23). To ascertain whether altered energy metabolism in *Akt1*$^{-/-}$ mice was a consequence of differences in body size, we measured the critical parameters in a cohort of WT and *Akt1*$^{-/-}$ mice with similar body weights and compositions (Fig. 5A). Once again, VO_2 and VCO_2 were elevated in *Akt1*$^{-/-}$ mice, although in this experiment the

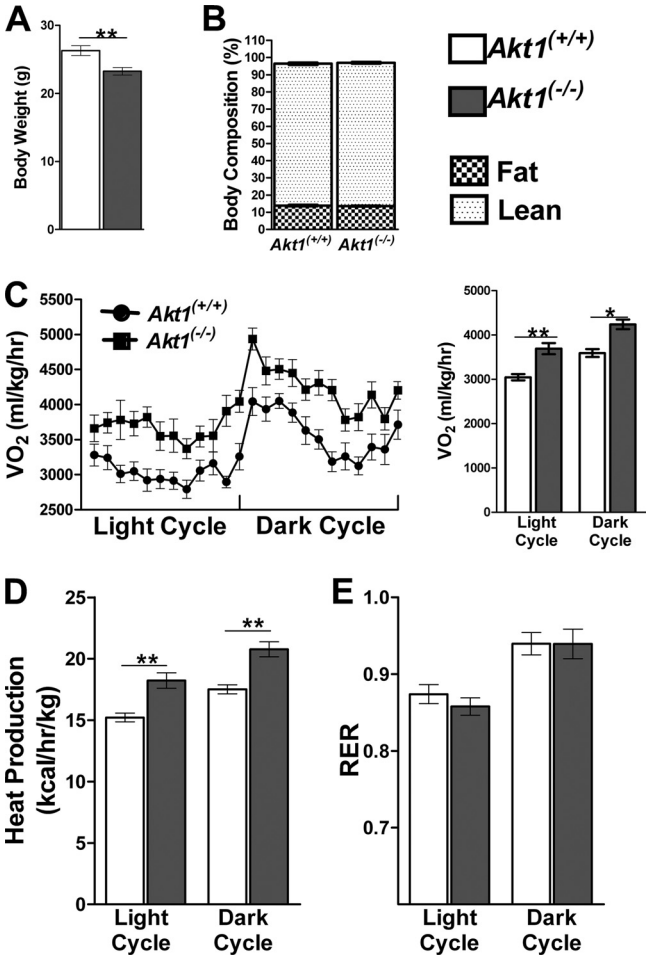

FIG 4 *Akt1*$^{-/-}$ mice displayed elevated energy expenditure compared to age-matched controls. (A) Body weights of WT and *Akt1*$^{-/-}$ mice. Both groups of mice were 10 weeks old and maintained on NC ($n = 10$ animals for each group). **, $P < 0.01$ by the Student t test. (B to E) Body composition based on NMR, O_2 consumption, heat production, and RER of WT and *Akt1*$^{-/-}$ mice fed NC ($n = 10$ animals for each group). *, $P < 0.05$; **, $P < 0.01$ by two-way ANOVA followed by the Bonferroni posttest. All data are presented as means ± SEM.

elevations were noted only during the dark period, when there was also an increase in heat production (Fig. 5B and C and data not shown). There were no significant changes in RER, locomotor activity, or food and water consumption (Fig. 5D and data not shown).

Given the elevated energy expenditure during the dark cycle for *Akt1*$^{-/-}$ mice in the previous experiment, we sought to accentuate this phenomenon further by subjecting the mice to a fasting-feeding regimen. WT and *Akt1*$^{-/-}$ mice of similar body weights were trained for 7 days under conditions in which during the light cycle food was removed, to generate a true "fasting" period, whereas mice had free access to food during the dark cycle ("feeding" period). As shown in Fig. 6A, body weights and compositions for this cohort were indistinguishable between WT and *Akt1*$^{-/-}$ mice. The amount of food and water consumed during the 24-h cycle was not different for the two genotypes (Fig. 6B). In this series of experiments, O_2 consumption was increased during both the light and dark cycles in *Akt1*$^{-/-}$ mice compared to weight-matched controls, and CO_2 production was also increased in the light cycle for these mice (Fig. 6C and data not shown). Heat production was also significantly increased in *Akt1*$^{-/-}$ mice (Fig. 6D). Moreover, *Akt1*$^{-/-}$ mice displayed decreased RER during the dark cycle and showed a similar trend during the light cycle compared to the weight-matched controls (Fig. 6E); also, in this experiment locomotor activity was enhanced during the dark cycle (Fig. 6F). These data indicate that the increased energy expenditure in *Akt1*$^{-/-}$ mice cannot be attributed to their reduced body size alone. Age-matched young *Akt1*$^{-/-}$ mice also showed the same phenotypes when subjected to the fasting-feeding protocol (data not shown).

Energy metabolism in skeletal muscle from *Akt1*$^{-/-}$ mice. Skeletal muscle contributes most of the energy expenditure in humans as well as in mice (4). One of the major determinants of VO_2 is the efficiency of coupling between mitochondrial respiration and ATP production (9, 10, 22). To ask whether alterations in coupling efficiency might account for the change in energetics in *Akt1*$^{-/-}$ mice, we assessed the expression levels of putative uncoupling proteins (UCPs) in skeletal muscle. *UCP3* mRNA levels were significantly increased in tibialis anterior (TA) and soleus muscles from *Akt1*$^{-/-}$ mice compared to age-matched controls, while *UCP2* showed similar trends (Fig. 7A). Using WT mice of a similar weight as controls, both *UCP2* and *UCP3* expression levels were increased in combined skeletal muscles of *Akt1*$^{-/-}$ mice (Fig. 7B). These differences persisted in the muscles of mice fed a high-fat diet (Fig. 7C). However, UCP3 protein levels were not significantly altered in TA or soleus muscles from *Akt1*$^{-/-}$ mice compared to the age-matched controls (Fig. 7D). In isolated skeletal muscle mitochondria, the state IV respiratory rate was the same between *Akt1*$^{-/-}$ mice and the age-matched controls (data not shown). Pyruvate dehydrogenase kinase 4 (PDK4) phosphorylates and inhibits the pyruvate dehydrogenase complex, resulting in a shift from oxidation of carbohydrates to oxidation of fat. Compared to age-matched controls fed a normal chow or high-fat diet, *Akt1*$^{-/-}$ mice had higher *PDK4* mRNA levels in skeletal muscles (Fig. 7A and C). Consistent with the gene expression pattern and reduced RER under some conditions, *ex vivo* palmitate oxidation was increased in soleus muscle samples from young *Akt1*$^{-/-}$ mice compared to age-matched controls (Fig. 7E); however, this difference was not seen in muscle samples from *Akt1*$^{-/-}$ mice compared to weight-matched controls (Fig. 7F).

Induction of *UCP1* in intramuscular brown adipocytes leads to protection from diet-induced obesity in mice (2); however, in these studies *UCP1* mRNA was not detected in muscle samples (data not shown). Elevated heat production was observed in *Akt1*$^{-/-}$ mice under most conditions; however, the expression levels of genes encoding uncoupling proteins or the coactivator PGC-1α (peroxisome proliferator-activated receptor gamma, coactivator 1α) in brown adipose tissue were not changed in either age-matched or weight-matched *Akt1*$^{-/-}$ mice fed a normal chow diet (Fig. 8A and B). The brown adipose tissue weights and core temperatures from *Akt1*$^{-/-}$ mice were not different than age-matched controls (Fig. 8C and D).

Two pathways recognized to regulate mitochondrial number, activity, and efficiency in muscle are those dependent on peroxisome proliferator-activated receptor δ (PPARδ) and AMP-activated protein kinase (AMPK) (1, 29, 36, 39). However, the expression levels of *PPARδ* and its targets, adipose differentiation-related protein (ADRP), forkhead box O1 (FoxO1), and PGC1α,

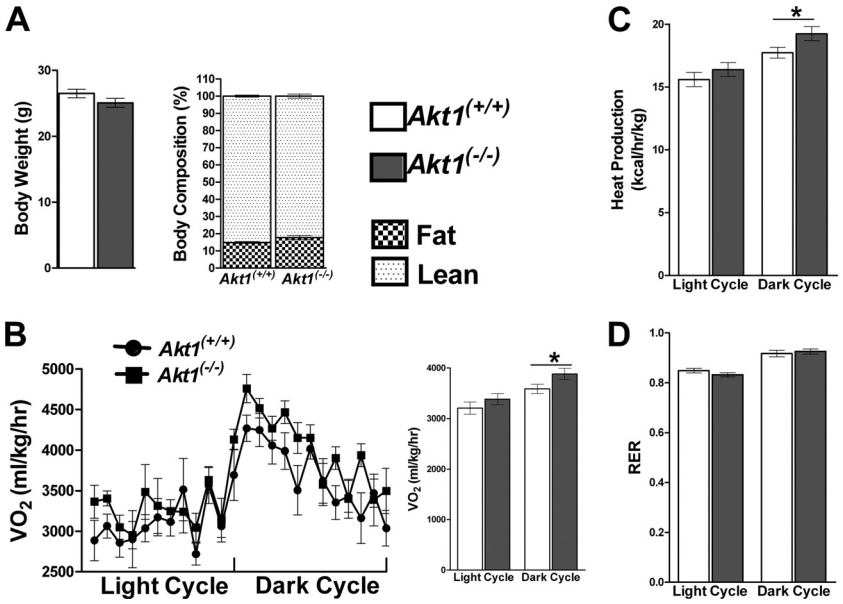

FIG 5 *Akt1*$^{-/-}$ mice displayed elevated energy expenditure compared to weight-matched controls. (A) Body weight and composition based on NMR analysis. WT mice were male and 10 weeks old, and *Akt1*$^{-/-}$ mice were 21 to 22 weeks old; all were maintained on NC. (B to D) O_2 consumption, heat production, and RER of *Akt1*$^{-/-}$ mice and weight-matched WT mice ($n = 5$ to 6 animals per group). *, $P < 0.05$ by two-way ANOVA followed by the Bonferroni posttest. All data are presented as means ± SEM.

were comparable in skeletal muscle from *Akt1*$^{-/-}$ and control mice (data not shown) (28, 29). Similarly, AMPK activation as assessed by phosphorylation of AMPK and its target, acetyl-coenzyme A carboxylase (ACC), was indistinguishable in soleus and TA muscles between *Akt1*$^{-/-}$ and WT mice (data not shown). Lastly, muscle citrate synthase activity, an indication of muscle mitochondrial number, was not altered by germ line deletion of *Akt1* (data not shown).

DISCUSSION

The recent epidemic of obesity and its associated conditions, cardiovascular diseases, cancer, and diabetes mellitus, has increased the demand for novel therapeutics targeted toward modulating appetite and/or energy metabolism. The search for clinically useful drugs has thus far met with limited success, and therefore the identification of novel potential targets remains of great interest. In this study, we showed that mice with germ line deletion of *Akt1* displayed many of the features one would desire in individuals treated with an ideal antiobesity drug: a mild increase in metabolic rate, prevention of both diet- and age-related obesity, and protection from insulin resistance.

The optimal strategies for measurement and presentation of energy expenditure in mice are controversial, particularly when comparing animals with different body weights and body compositions (4, 23). Use of age-matched animals might overestimate the metabolic rate for mice with lower body weights, while comparing weight-matched animals might introduce artifacts related to aging, which leads to muscle mass loss and compromised mitochondrial function (30). This issue is particularly challenging when studying *Akt1*$^{-/-}$ mice on a C57BL/6J background, since these mice are born about 20% smaller than WT mice and remain so for life (6, 8). In order to be certain of the energetic effects of loss of *Akt1*, we used two approaches: (i) we compared *Akt1*$^{-/-}$ mice to control mice under as many conditions as feasible and (ii) we tried to dissociate the changes in body size from the body size by generating mice with tissue-specific loss of *Akt1*. Regarding the first approach, we compared the energy expenditures of *Akt1*$^{-/-}$ mice to age-matched as well as weight-matched controls, and we observed consistent outcomes for almost all assays. Although there were some quantitative differences, e.g., *Akt1*$^{-/-}$ mice showed milder effects on O_2 consumption and CO_2 production than weight-matched as opposed to age-matched mice (Fig. 4 and 5), the qualitative alterations were consistent. We also studied the mice under defined feeding conditions, in which they were deprived of food during the light cycle. In these experiments, once again the increase in metabolic rate in the *Akt1*$^{-/-}$ mice was evident independently of control group and, surprisingly, there was also higher locomotor activity during the dark cycle in the *Akt1*$^{-/-}$ mice (Fig. 6 and data not shown). In addition to age and size, body composition influences energy expenditure, and there is no consensus on the best normalization tool to use when expressing VO_2 or VCO_2 (4, 23). Under conditions of normal chow feeding, the body compositions of WT and *Akt1*$^{-/-}$ mice were indistinguishable, and thus energy expenditure values were similar when normalized to either body weight or lean mass. In the HFD studies, normalization of energy expenditure to body weight or to lean mass showed an increased VO_2 in *Akt1*$^{-/-}$ mice (Fig. 1C), and so the choice of the correct normalization parameter was not an issue. To exclude the remote possibility that these phenotypes were caused by a locus or loci tightly linked to *Akt1*, we generated an independent *Akt1*$^{-/-}$ mouse line by breeding *Akt1*$^{lox/lox}$ mice to *EIIa* > *Cre* mice. These mice behaved similar to the original line generated: smaller body size and increased energy expenditure on a normal chow diet, an elevated energy expenditure, and protection from obesity when fed am HFD (Fig. 1F to I and data not shown). Interestingly, in the newly derived line, *Akt1*$^{+/-}$ mice displayed intermediate effects for most metabolic

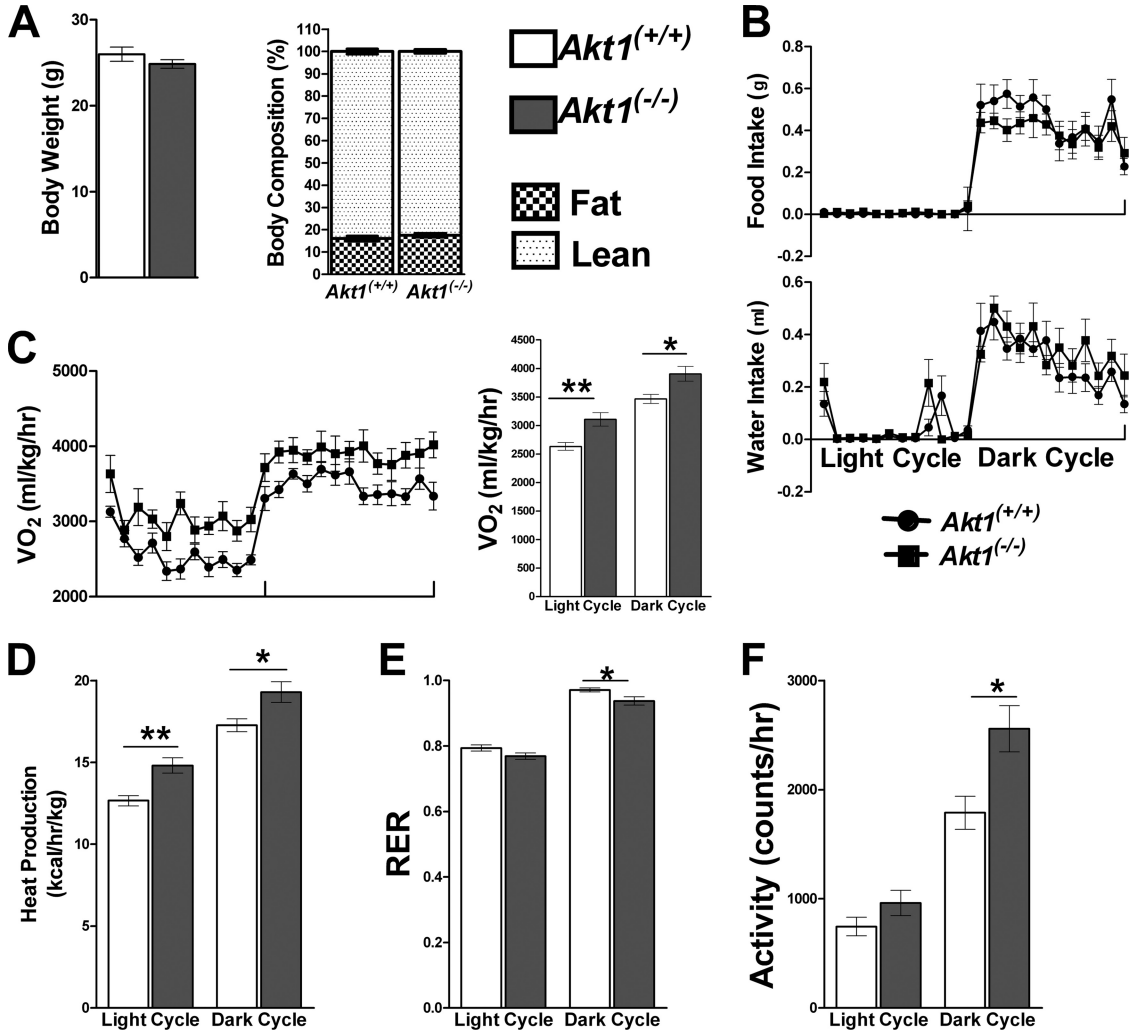

FIG 6 *Akt1*$^{-/-}$ mice exhibited higher energy expenditures than weight-matched WT mice during controlled feeding. (A) Body weight and composition by NMR. WT mice were 10 weeks old, and *Akt1*$^{-/-}$ mice were 21 to 22 weeks old. (B to F) Food and water consumption, O_2 consumption, heat production, RER, and locomotor activity of *Akt1*$^{-/-}$ mice and weight-matched WT mice. All mice were maintained on NC, and food was removed during the light cycle and provided during the dark cycle ($n = 10$ to 12 animals per group). *, $P < 0.05$; **, $P < 0.01$ by two-way ANOVA followed by the Bonferroni posttest. All data are presented as means ± SEM.

parameters (Fig. 1G to I), suggesting that Akt1 is regulatory and not just permissive in the control of energy metabolism. The slight quantitative differences in phenotypes between the two mouse lines were almost certainly due to their distinct genetic backgrounds. Lastly, we were unable to reproduce the increased VO_2 and VCO_2 in mice by deleting *Akt1* selectively in brain, muscle, or liver tissue (Fig. 2 and data not shown); whereas these data did not allow dissociation of energy expenditure from body size, they suggested strongly that the increased metabolic rate is cell nonautonomous in muscle.

Lean mass, which is primarily skeletal muscle, contributes most of the energy expenditure during both rest and exercise (4). Several studies using mouse genetics have suggested that increasing mitochondria biogenesis in skeletal muscle leads to increased energy expenditure and protection from diet-induced obesity in mice (1, 29, 36, 39). Increased mitochondrial mass alone with preservation of normal function would be unlikely to influence metabolic rate, and in fact these genetic models also reveal increased expression of *UCP3* and *PDK4* in skeletal muscle (29, 39). Skeletal muscle from *Akt1*$^{-/-}$ mice had an increase in *UCP3* mRNA comparable to that in transgenic mice protected from increases in adiposity, but there were no changes in the UCP3 protein. Consistent with this observation, the coupling efficiency was unchanged in isolated mitochondria from *Akt1*$^{-/-}$ skeletal muscle. Induction of UCP1, which is the major uncoupling protein in brown adipose tissue, in intramuscular brown adipocytes increases energy expenditure and prevents diet-induced obesity in mice (2); however, we did not observe increases in *UCP1* in muscles or brown adipose tissue from *Akt1*$^{-/-}$ mice (Fig. 8A and B and data not shown). Phosphorylation of the canonical Akt target Forkhead box O 1 in brain and skeletal muscle was not altered in *Akt1*$^{-/-}$ mice compared to controls (data not shown), suggesting that this transcription factor is unlikely to be responsible for the energy expenditure phenotypes (17).

Mice deficient for Akt1 showed an elevation in the expression *PDK4* as well as *UCP3* in skeletal muscle (Fig. 7). PDK4, the major

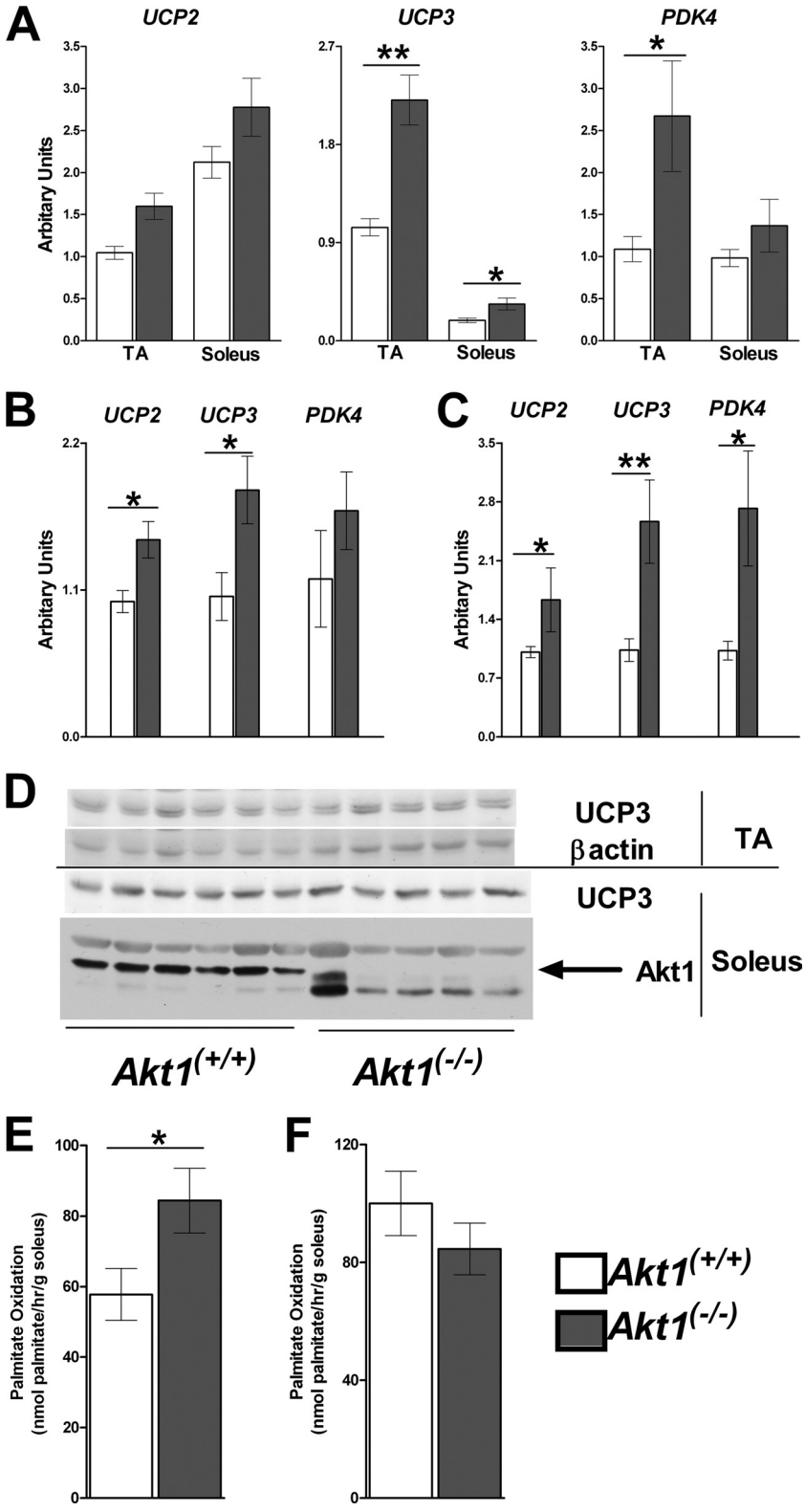

FIG 7 Increased fatty acid oxidation in skeletal muscle from *Akt1*$^{-/-}$ mice. (A) *UCP2*, *UCP3*, and *PDK4* expression in skeletal muscles of age-matched young WT and *Akt1*$^{-/-}$ mice. Mice are as described for Fig. 3 ($n = 10$ for each group). (B) *UCP2*, *UCP3*, and *PDK4* expression levels in skeletal muscles of weight-matched WT and *Akt1*$^{-/-}$ mice. Mice are as described for Fig. 4 ($n = 5$ to 6 animals for each group). (C) *UCP2*, *UCP3*, and *PDK4* expression levels in skeletal muscles of HFD-fed WT and *Akt1*$^{-/-}$ mice. Mice are as described for Fig. 1 ($n = 4$ to 5 animals for each group). (D) Western blot for UCP3 in muscles from age-matched WT and *Akt1*$^{-/-}$ mice. (E) Palmitate oxidation rate of isolated soleus muscles from age-matched WT and *Akt1*$^{-/-}$ mice. Both WT and *Akt1*$^{-/-}$ mice were 10 weeks old and were fed NC ($n = 5$ to 6 for each genotype). (F) Palmitate oxidation rate of isolated soleus muscles from weight-matched WT and *Akt1*$^{-/-}$ mice. WT mice were 10 weeks old, and *Akt1*$^{-/-}$ mice were 22 weeks old. All mice were fed NC ($n = 5$ for each genotype). *, $P < 0.05$; **, $P < 0.01$ by the Student *t* test. All data are presented as means ± SEM.

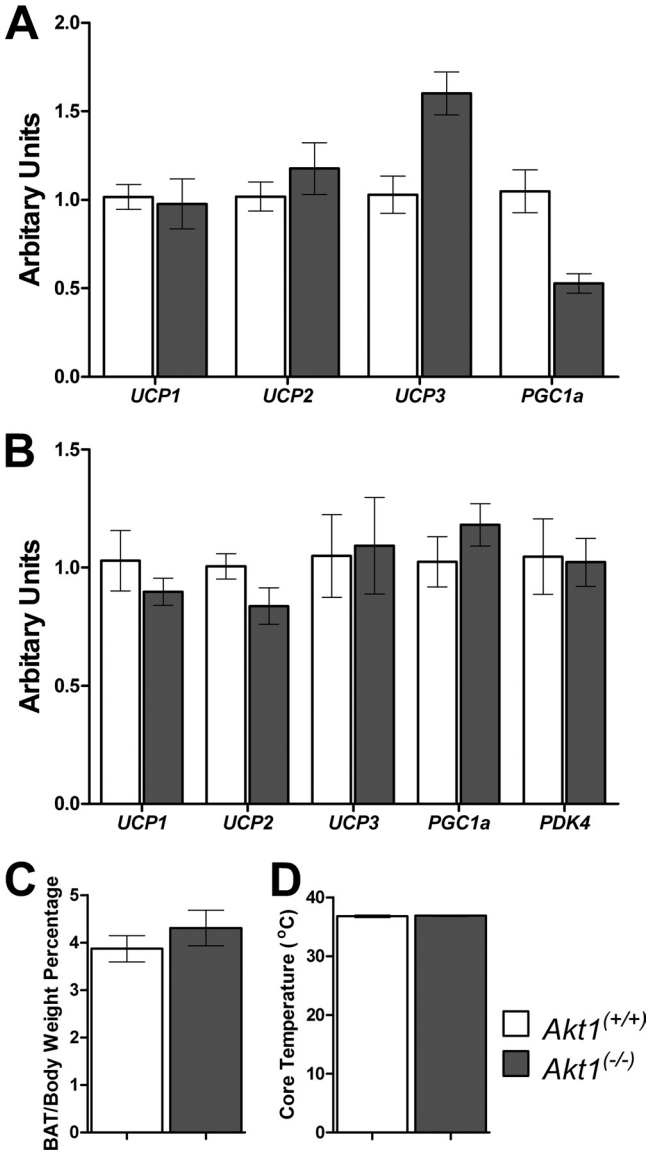

FIG 8 mRNA levels of uncoupling proteins are not altered in brown adipose tissue from *Akt1*$^{-/-}$ mice. (A) *UCP1*, *UCP2*, *UCP3*, and *PGC1α* expression in brown adipose tissue of age-matched young WT and *Akt1*$^{-/-}$ mice. Mice are as described for Fig. 3 ($n = 7$ for each group). (B) *UCP1*, *UCP2*, *UCP3*, *PGC1α*, and *PDK4* expression in brown adipose tissue of weight-matched WT and *Akt1*$^{-/-}$ mice. Mice are as described for Fig. 4 ($n = 5$ to 6 animals for each group). (C and D) Brown adipose tissue (BAT) weight percentage of body weight and core temperature of age-matched young WT and *Akt1*$^{-/-}$ mice ($n = 5$ to 6 animals for each group). All data are presented as means ± SEM.

isoform in muscle, phosphorylates and suppresses the activity of the pyruvate dehydrogenase complex, which converts carbohydrate-derived pyruvate into acetyl coenzyme A (32). This has the effect of promoting fatty acid oxidation relative to carbohydrates. *UCP3* and *PDK4* are often coregulated as part of the transition to fatty acid oxidation, most notably during fasting or HFD feeding, but also upon exercise (21, 32–34). Coordinate increases in *UCP3* and *PDK4* expression levels in skeletal muscle also result from genetic manipulations that promote mitochondrial biogenesis (29, 39). Activation of PPARδ by overexpression or agonist treatment induces *UCP3* and *PDK4* expression levels and mitochondrial biogenesis, and it increases oxidative fiber composition, possibly through activation of AMPK (29, 39). Loss of *S6K1* in mice results in increased muscle mitochondrial content, elevated energy expenditure, and protection from diet-induced obesity, an effect also linked to activation of AMPK in skeletal muscle (1, 36). We did not observe increases in mitochondrial content or activation of AMPK and PPARδ in skeletal muscle from *Akt1*$^{-/-}$ mice; in addition, the modest decreases in the cross-sectional areas of both type I and type II muscle fibers in *Akt1*$^{-/-}$ mice are proportional to body size (15).

It was reported recently that 5- to 6-month-old *Akt1*$^{-/-}$ mice, which were generated independently by another laboratory, had decreased blood glucose levels, improved glucose tolerance, and insulin sensitivity (5). A primary effect on pancreatic β-cells and abnormal insulin secretion was suggested to be responsible for most of this phenotype, although improved insulin sensitivity was also reported (5). We did not find differences in serum insulin levels in young *Akt1*$^{-/-}$ mice (8), and insulin levels tended to be lower in *Akt1*$^{-/-}$ mice after HFD feeding (Table 1). It is likely that the decrease in insulin resistance described by Buzzi et al. was secondary to increased energy expenditure and prevention of the increased adipose mass that normally accompanies aging.

In this study, we identified a novel function of Akt1 in the control of energy metabolism. Most tantalizing, the data reported here suggest that Akt1 might be a reasonable target for therapeutics aimed at the prevention of obesity. Compounds with relative specificity for individual Akt isoforms have already been developed (3, 26, 42). An important question is whether the isoform-specific roles of the Akt family in mice are recapitulated in humans; a recent report describing an association between an AKT1 gene G205T (rs1130214) polymorphism and VO_2 in humans has suggested that this is the case (27).

ACKNOWLEDGMENTS

This work was supported by NIH grants RO1 DK56886 and PO1 DK49210 to M.J.B. The Mouse Phenotyping, Physiology and Metabolism Core and the Radioimmunoassay and Biomarker Core were supported by the Diabetes and Endocrinology Research Center, University of Pennsylvania (NIH DK-19525).

We thank Mary Selak, The Children's Hospital of Philadelphia, for help and suggestions on muscle mitochondrial analysis, and Ravindra Dhir, University of Pennsylvania, for suggestions on energy expenditure measurements and *ex vivo* fatty acid oxidation measurements.

REFERENCES

1. **Aguilar V, et al.** 2007. S6 kinase deletion suppresses muscle growth adaptations to nutrient availability by activating AMP kinase. Cell Metab. **5**:476–487.
2. **Almind K, Manieri M, Sivitz WI, Cinti S, Kahn CR.** 2007. Ectopic brown adipose tissue in muscle provides a mechanism for differences in risk of metabolic syndrome in mice. Proc. Natl. Acad. Sci. U. S. A. **104**: 2366–2371.
3. **Barnett SF, et al.** 2005. Identification and characterization of pleckstrin-homology-domain-dependent and isoenzyme-specific Akt inhibitors. Biochem. J. **385**:399–408.
4. **Butler AA, Kozak LP.** 2010. A recurring problem with the analysis of energy expenditure in genetic models expressing lean and obese phenotypes. Diabetes **59**:323–329.
5. **Buzzi F, et al.** 2010. Differential effects of protein kinase B/Akt isoforms on glucose homeostasis and islet mass. Mol. Cell. Biol. **30**:601–612.
6. **Chen WS, et al.** 2001. Growth retardation and increased apoptosis in mice with homozygous disruption of the Akt1 gene. Genes Dev. **15**: 2203–2208.
7. **Cho H, et al.** 2001. Insulin resistance and a diabetes mellitus-like syn-

drome in mice lacking the protein kinase Akt2 (PKB beta). Science **292**: 1728–1731.
8. **Cho H, Thorvaldsen JL, Chu Q, Feng F, Birnbaum MJ.** 2001. Akt1/PKBα is required for normal growth but dispensable for maintenance of glucose homeostasis in mice. J. Biol. Chem. **276**:38349–38352.
9. **Choi CS, et al.** 2007. Overexpression of uncoupling protein 3 in skeletal muscle protects against fat-induced insulin resistance. J. Clin. Invest. **117**: 1995–2003.
10. **Clapham JC, et al.** 2000. Mice overexpressing human uncoupling protein-3 in skeletal muscle are hyperphagic and lean. Nature **406**: 415–418.
11. **Costford SR, Chaudhry SN, Crawford SA, Salkhordeh M, Harper ME.** 2008. Long-term high-fat feeding induces greater fat storage in mice lacking UCP3. Am. J. Physiol. Endocrinol. Metab. **295**:E1018–E1024.
12. **Dummler B, et al.** 2006. Life with a single isoform of Akt: mice lacking Akt2 and Akt3 are viable but display impaired glucose homeostasis and growth deficiencies. Mol. Cell. Biol. **26**:8042–8051.
13. **Easton RM, et al.** 2005. Role for Akt3/protein kinase Bγ in attainment of normal brain size. Mol. Cell. Biol. **25**:1869–1878.
14. **Garofalo RS, et al.** 2003. Severe diabetes, age-dependent loss of adipose tissue, and mild growth deficiency in mice lacking Akt2/PKB beta. J. Clin. Invest. **112**:197–208.
15. **Goncalves MD, et al.** 2010. Akt deficiency attenuates muscle size and function but not the response to ActRIIB inhibition. PLoS One **5**:e12707.
16. **Gonzalez E, McGraw TE.** 2009. The Akt kinases: isoform specificity in metabolism and cancer. Cell Cycle **8**:2502–2508.
17. **Gross DN, Wan M, Birnbaum MJ.** 2009. The role of FOXO in the regulation of metabolism. Curr. Diab. Rep. **9**:208–214.
18. **Guan HP, Goldstein JL, Brown MS, Liang G.** 2009. Accelerated fatty acid oxidation in muscle averts fasting-induced hepatic steatosis in SJL/J mice. J. Biol. Chem. **284**:24644–24652.
19. **Hamilton MT, Hamilton DG, Zderic TW.** 2007. Role of low energy expenditure and sitting in obesity, metabolic syndrome, type 2 diabetes, and cardiovascular disease. Diabetes **56**:2655–2667.
20. **He L, et al.** 2010. The critical role of AKT2 in hepatic steatosis induced by PTEN loss. Am. J. Pathol. **176**:2302–2308.
21. **Hildebrandt AL, Pilegaard H, Neufer PD.** 2003. Differential transcriptional activation of select metabolic genes in response to variations in exercise intensity and duration. Am. J. Physiol. Endocrinol. Metab. **285**: E1021–E1027.
22. **Horvath TL, et al.** 2003. Uncoupling proteins-2 and 3 influence obesity and inflammation in transgenic mice. Int. J. Obes. Relat. Metab. Disord. **27**:433–442.
23. **Kaiyala KJ, et al.** 2010. Identification of body fat mass as a major determinant of metabolic rate in mice. Diabetes **59**:1657–1666.
24. **Leavens KF, Easton RM, Shulman GI, Previs SF, Birnbaum MJ.** 2009. Akt2 is required for hepatic lipid accumulation in models of insulin resistance. Cell Metab. **10**:405–418.
25. **Le Lay J, et al.** 2009. CRTC2 (TORC2) contributes to the transcriptional response to fasting in the liver but is not required for the maintenance of glucose homeostasis. Cell Metab. **10**:55–62.
26. **Lindsley CW, et al.** 2005. Allosteric Akt (PKB) inhibitors: discovery and SAR of isozyme selective inhibitors. Bioorg. Med. Chem. Lett. **15**:761–764.
27. **McKenzie JA, Witkowski S, Ludlow AT, Roth SM, Hagberg JM.** 2011. AKT1 G205T genotype influences obesity-related metabolic phenotypes and their responses to aerobic exercise training in older Caucasians. Exp. Physiol. **96**:338–347.
28. **Nahle Z, et al.** 2008. CD36-dependent regulation of muscle FoxO1 and PDK4 in the PPAR delta/beta-mediated adaptation to metabolic stress. J. Biol. Chem. **283**:14317–14326.
29. **Narkar VA, et al.** 2008. AMPK and PPARδ agonists are exercise mimetics. Cell **134**:405–415.
30. **Paradies G, Petrosillo G, Paradies V, Ruggiero FM.** 2010. Oxidative stress, mitochondrial bioenergetics, and cardiolipin in aging. Free Radic. Biol. Med. **48**:1286–1295.
31. **Peng XD, et al.** 2003. Dwarfism, impaired skin development, skeletal muscle atrophy, delayed bone development, and impeded adipogenesis in mice lacking Akt1 and Akt2. Genes Dev. **17**:1352–1365.
32. **Pilegaard H, Neufer PD.** 2004. Transcriptional regulation of pyruvate dehydrogenase kinase 4 in skeletal muscle during and after exercise. Proc. Nutr. Soc. **63**:221–226.
33. **Samec S, Seydoux J, Dulloo AG.** 1999. Post-starvation gene expression of skeletal muscle uncoupling protein 2 and uncoupling protein 3 in response to dietary fat levels and fatty acid composition: a link with insulin resistance. Diabetes **48**:436–441.
34. **Samec S, Seydoux J, Dulloo AG.** 1998. Role of UCP homologues in skeletal muscles and brown adipose tissue: mediators of thermogenesis or regulators of lipids as fuel substrate? FASEB J. **12**:715–724.
35. **Slentz CA, Houmard JA, Kraus WE.** 2009. Exercise, abdominal obesity, skeletal muscle, and metabolic risk: evidence for a dose response. Obesity (Silver Spring) **17**(Suppl. 3):S27–S33.
36. **Um SH, et al.** 2004. Absence of S6K1 protects against age- and diet-induced obesity while enhancing insulin sensitivity. Nature **431**:200–205.
37. **Venables MC, Jeukendrup AE.** 2009. Physical inactivity and obesity: links with insulin resistance and type 2 diabetes mellitus. Diabetes Metab. Res. Rev. **25**(Suppl. 1):S18–S23.
38. **Wan M, et al.** 2011. Postprandial hepatic lipid metabolism requires signaling through Akt2 independent of the transcription factors FoxA2, FoxO1 and SREBP1c. Cell Metab. **14**:516–527.
39. **Wang YX, et al.** 2004. Regulation of muscle fiber type and running endurance by PPARδ. PLoS Biol. **2**:e294.
40. **Whiteman EL, Cho H, Birnbaum MJ.** 2002. Role of Akt/protein kinase B in metabolism. Trends Endocrinol. Metab. **13**:444–451.
41. **Yang ZZ, et al.** 2005. Dosage-dependent effects of Akt1/protein kinase Bα (PKBα) and Akt3/PKBγ on thymus, skin, and cardiovascular and nervous system development in mice. Mol. Cell. Biol. **25**:10407–10418.
42. **Zhao Z, et al.** 2008. Development of potent, allosteric dual Akt1 and Akt2 inhibitors with improved physical properties and cell activity. Bioorg. Med. Chem. Lett. **18**:49–53.